Nanoscale Horizons

ROYAL SOCIETY OF CHEMISTRY

COMMUNICATION

View Article Online
View Journal | View Issue

Cite this: *Nanoscale Horiz.*, 2025, **10**, 3369

Received 8th July 2025,
Accepted 10th September 2025

DOI: 10.1039/d5nh00468c

rsc.li/nanoscale-horizons

Light-triggered quenching of the ^{19}F-MRI signal from micelle-encapsulated PERFECTA

Claire Leterrier, [a] Guillaume Pinna, [bc] Marie Vandamme, [bc] Mélissa Glatigny, [d] Erwan Selingue, [d] Françoise Geffroy, [d] Sébastien Mériaux, *[d] Edmond Gravel *[a] and Eric Doris *[a]

We report the development of a fluorinated micellar nanosystem whose ^{19}F-MRI signal can be selectively dimmed by application of an external stimulus. A photo-activatable quencher unit (ferrocene) was co-encapsulated with the superfluorinated PERFECTA probe in colloidal micelles. While pristine micelles were MRI responsive ("On" state), their irradiation by light triggered the "Off" MRI-state of PERFECTA.

New concepts

A light-activated switch was designed to enable controlled extinction of the ^{19}F-MRI signal from a micellar nanocarrier containing a MRI-responsive superfluorinated probe (PERFECTA) and a photo-activatable ferrocene quencher. Upon illumination, the ferrocene is converted into paramagnetic ferrocenium, which shortens the T_2 relaxation time of nearby ^{19}F nuclei, effectively silencing the MRI signal. Unlike most activatable ^{19}F-MRI probes, which operate from an "off" to "on" transition, our method switches-off MRI signals on demand, and this phenomenon is triggered for the first time by light. The co-encapsulation of a photo-activatable quencher unit and a superfluorinated probe within micellar nanocarriers provided the requisite proximity and confinement for effective paramagnetic resonance enhancement effect-mediated signal attenuation of PERFECTA. This light-responsive signal modulation introduces a novel approach to MRI contrast enhancement that could enable selective signal dimming in extraneous tissues, thus improving delineation of pathological sites in clinical practice. Proof of concept was established using a rodent model.

1. Introduction

Magnetic resonance imaging (MRI) is a noninvasive technique that enables high-spatial resolution imaging of deep soft tissues, without exposing patients to ionizing radiation. Conventional ^{1}H-MRI generates contrasted images based on the variable relaxation rates of water protons depending on their environment.[1] When the contrast between healthy and pathological tissues is low, the administration of agents capable of modifying relaxation rates of neighboring protons, *e.g.* paramagnetic gadolinium(III)[2] or superparamagnetic iron oxide nanoparticles,[3] may prove useful. Despite their effectiveness, these contrast agents are detected indirectly *via* changes in the magnetic resonance signals of the surrounding water.

On the other hand, contrast agents incorporating responsive atoms such as ^{13}C, ^{31}P, ^{17}O or ^{19}F, can be directly observed by magnetic resonance techniques, guaranteeing signal specificity and ease of quantification.[4] In this case, the agents themselves are imaged, enabling absolute quantification of the MRI signal, which is proportional to the probe concentration. In the context of *in vivo* quantitative imaging, fluorine-19 is a promising nucleus,[5] which benefits from 100% natural abundance, spin $\frac{1}{2}$, high nuclear receptivity,[6] and low background noise as virtually no endogenous fluorine is found in living bodies.

When designing ^{19}F-MRI probes, the number and nature of fluorine atoms must be taken into account. PERFECTA is one of the few ^{19}F probes currently available in the literature.[7] It is a symmetrical molecule with 36 chemically equivalent fluorine atoms, all resonating at the same frequency and providing a unique and strong magnetic resonance signal.[8] However, PERFECTA is not water-soluble, and if it is to be used in biomedical applications, it must be formulated so that it can be dispersed in aqueous medium prior to administration.[9–12]

Our group has long been involved in the development of nanometric carrier systems for drug delivery and imaging applications.[13–24] We recently reported the design of fluorinated micelles for the encapsulation and biocompatibilization of PERFECTA, applied to *in vivo* ^{19}F-MRI detection of tumors.[25] These micelles consist of supramolecular aggregates of PFTD-PEG amphiphilic units comprising: (i) a perfluorinated chain

[a] *CEA, INRAE, Département Médicaments et Technologies pour la Santé (DMTS), SCBM, Université Paris-Saclay, 91191 Gif-sur-Yvette, France. E-mail: edmond.gravel@cea.fr, eric.doris@cea.fr*
[b] *CEA, Stabilité Génétique Cellules Souches et Radiations, Université Paris Cité, Plateforme PARi, 92260 Fontenay-aux-Roses, France*
[c] *CEA, Stabilité Génétique Cellules Souches et Radiations, Université Paris-Saclay, Plateforme PARi, 92260 Fontenay-aux-Roses, France*
[d] *CEA, CNRS, BAOBAB, NeuroSpin, Université Paris-Saclay, 91191 Gif-sur-Yvette, France. E-mail: sebastien.meriaux@cea.fr*

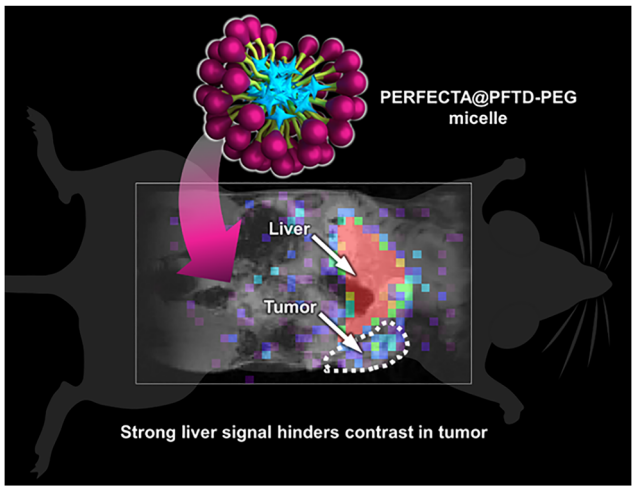

Fig. 1 Illustration of PERFECTA-loaded micelles and previous *in vivo* ^{19}F-MR imaging of PERFECTA@PFTD-PEG 96 h after intravenous injection of the micelles to a tumor-bearing mouse.

forming the central hydrophobic core of the micelle and designed to accommodate fluorinated probes; and (ii) a hydrophilic poly(ethylene glycol) (PEG, MW = 2000) head group forming the outer hydrophilic layer and designed to delay adsorption of plasma proteins and prevent rapid opsonisation/elimination *in vivo*.[26] In the context of cancer diagnosis, we evaluated PERFECTA-loaded micelles (PERFECTA@PFTD-PEG micelles) in a mouse model for their ability to passively target tumors through the enhanced permeability and retention (EPR) effect. Micelles were intravenously injected to MC38 tumor-bearing mice and were found to selectively accumulate (>3.5% of the injected dose) in the tumor area, as evidenced and quantified by ^{19}F-MR imaging. Yet, preclinical imaging performance was somewhat impaired by the non-specific accumulation of micelles in the liver, resulting in a strong MRI signal in the abdomen and reducing the contrast in the area of interest (*i.e.* the tumor, Fig. 1).

To selectively improve the contrast-to-noise ratio of the pathological site, we conceived that selective attenuation of the MRI signal in non-pathological liver tissue should facilitate the visualization of the tumor zone. With this feature in mind, we have developed a micellar ^{19}F-MRI probe whose signal can be selectively dimmed in chosen areas (those not to be imaged) by application of an external stimulus. We selected the ferrocenyl group as the quencher unit to be associated to PERFECTA-loaded micelles. In fact, some ferrocene derivatives can be activated by light[27] and converted to higher oxidation state ferroceniums.[28] Since the latter possesses paramagnetic properties, capable of interfering with the magnetic resonance response of the observed nuclei, we sought to exploit the light-triggered transition from ferrocene to ferrocenium to selectively attenuate the ^{19}F-MRI signals of PERFECTA micelles, in a controlled manner.

2. Results

Our approach relied on the aqueous assembly of fluorinated micelles that were loaded with both PERFECTA and a ferrocene derivative. In its initial state, and in the absence of light, the diamagnetic ferrocene incorporated within the micelle should not interfere with the signal of PERFECTA, therefore allowing regular ^{19}F-MRI visualization of the probe (“On” state). However, upon activation by light, the ferrocenyl unit will be photo-oxidized. In fact, while pristine ferrocene is mostly photostable, acyl-substituted ferrocenes are prone to photo-oxidation into the corresponding ferroceniums.[29,30] Due to the paramagnetic nature of the latter, relaxation times of nearby ^{19}F nuclei will be affected, resulting in a likely attenuation of the MRI signals of PERFECTA (“Off” state).

2.1. Preliminary evaluation: assembly of PERFECTA@PFTD-PEG micelles and MRI studies

Simple ^{19}F-MRI responsive micelles (without ferrocene) were assembled from fluorinated PFTD-PEG amphiphiles (synthesized in two steps from commercially available precursors), by sonication in water in the presence of solid PERFECTA. This resulted, after filtration, in a stable homogeneous aqueous dispersion of PERFECTA@PFTD-PEG micelles. ^{19}F-NMR quantification in the presence of an internal standard indicated a probe loading of *ca.* 40 wt% in the micelles (13.5 mg of PERFECTA in 20 mg of PFTD-PEG micelles per mL of water (encapsulation efficiency = 68%), [PERFECTA] = 13.3 mM). The PERFECTA-loaded micelles had a mean hydrodynamic diameter of 20 nm, as measured by dynamic light scattering (DLS) experiments and a zeta potential near 0 mV (Fig. S1). ^{19}F-MRI characterization of the micelle payload was performed by acquiring images of tubes filled with different formulations of PERFECTA@PFTD-PEG micelles dispersed in water, using a 7 T preclinical scanner and a Multi-Slice Multi-Echo (MSME) sequence. To establish an optimal imaging protocol in terms of detection threshold, decreasing concentrations of PERFECTA (from 13.3 mM to 0 mM) in PFTD-PEG micelles (20 mg mL^{-1}) were imaged. The MSME sequence offered a suitable detection threshold of approximately 2 mM, confirming the potential of PERFECTA-loaded micelles for ^{19}F-MRI (Fig. 2).

2.2. Synthesis and encapsulation of the ferrocenyl quencher unit

We next investigated the micellar co-encapsulation of PERFECTA together with a ferrocenyl unit capable of being photo-activated to trigger the “Off” state of the ^{19}F-MRI signal. To make the ferrocene derivative suitable for encapsulation in the core of PFTD-PEG micelles, it was derivatized with two fluorinated chains to impart a fluorophilic character to the probe (Scheme 1). The synthesis of

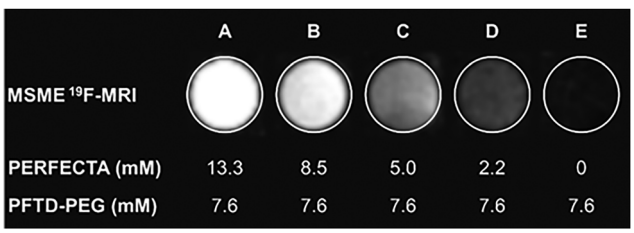

Fig. 2 Multi-slice multi-echo (MSME) sequence for ^{19}F-MR imaging of PFTD-PEG micelles containing various concentrations of PERFECTA.

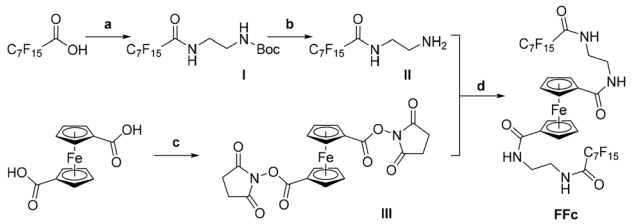

Scheme 1 Synthesis of fluorinated ferrocene (FFc): (a) *N*-methyl morpholine, isobutyl chloroformate, *N*-Boc ethylenediamine, THF; (b) HCl in dioxane, THF; (c) EDC·HCl, NHS, DMF; (d) NEt_3, $CHCl_3$.

the fluorinated ferrocenyl unit started with the coupling of perfluorooctanoic acid to monoprotected ethylene diamine (Scheme 1, step a, compound **I**). The protecting Boc group was subsequently removed under acidic conditions (step b, compound **II**), before the resulting primary amine was reacted (step d) with 1,1′-ferrocene dicarboxylic acid previously activated as succinimidyl esters (step c, compound **III**). The fluorinated ferrocene (FFc) was obtained as a pale-yellow solid.

Mixed FFc/PERFECTA@PFTD-PEG micelles were produced by co-encapsulation of PERFECTA and FFc in the presence of PFTD-PEG amphiphiles, under ultrasonic activation (Fig. 3). It is worth noting that PERFECTA loading remained constant at 13.5 mg mL^{-1}, while the FFc load reached a maximum of 5 mg mL^{-1}, as measured by NMR experiments (encapsulation efficiency = 100%). Stability tests indicated that micelles were stable over several weeks at room temperature, as neither precipitation nor leaching of the payload was observed.

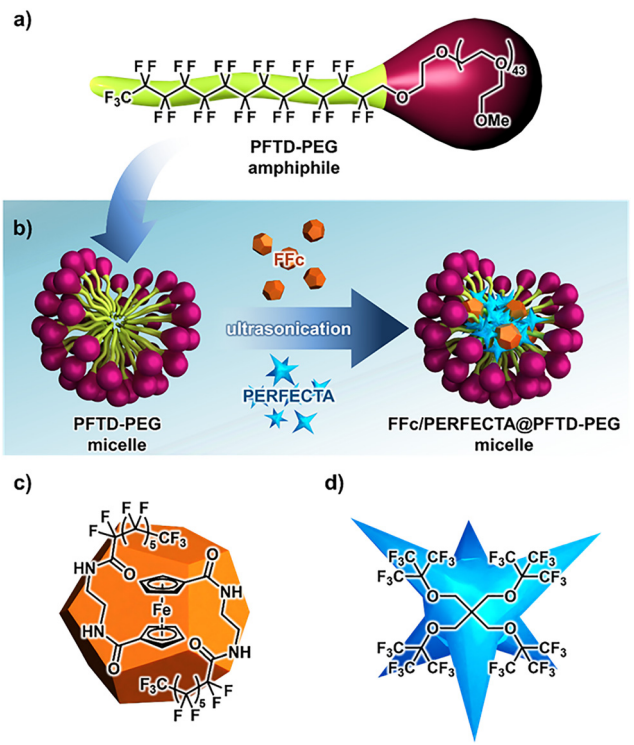

Fig. 3 (a) Structure of PFTD-PEG; (b) assembly of PFTD-PEG micelles and co-encapsulation of PERFECTA and FFc; (c) structure of FFc; (d) structure of PERFECTA.

2.3. Photo-activation studies of FFc/PERFECTA@PFTD-PEG micelles

In order to determine the optimal wavelength for the photo-triggered ferrocene to ferrocenium oxidative shift, UV-visible spectra of micelles encapsulating both PERFECTA and FFc were recorded in water (Fig. 4a). We observed a major absorption band between 410 and 480 nm that was ascribed to charge transfer between iron and cyclopentadienyl rings, giving the ferrocenyl compound its characteristic yellowish color. The FFc/PERFECTA@PFTD-PEG micellar solution was thereafter irradiated with a light-emitting diode (LED) source at 460 nm. After 30 s of illumination, we detected a marked decrease of the 450 nm-centered absorption band, which fully vanished after 2 min of exposure to light. This decrease was accompanied by a change in color of the colloidal suspension, from yellowish to brownish, suggesting a chemical modification of the ferrocenyl group and its oxidation to ferrocenium (Fig. 4b). Of note, the colloidal suspension remained stable over time although ferrocenium can decompose by reaction with nucleophiles such as water. This observation suggests that the hydrophobic ferrocenyl group remains encapsulated in the lipophilic micelle core after photo-oxidation and is protected from the surrounding water.

2.4. MRI response of FFc/PERFECTA@PFTD-PEG micelles in their "On" and "Off" states

^{19}F-MRI characterization of the mixed micelle was performed by acquiring images of tubes filled with different formulations of FFc/PERFECTA@PFTD-PEG micelles dispersed in water, using a 7 T preclinical scanner and a MSME sequence. Tubes

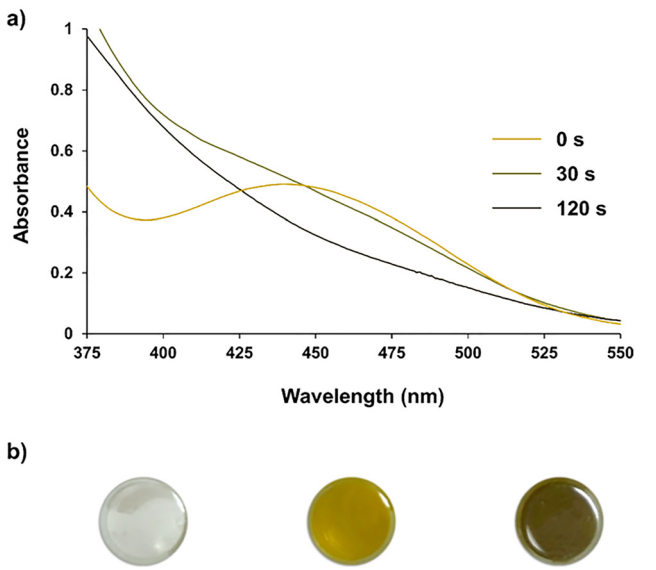

Fig. 4 Photo-activation of FFc/PERFECTA@PFTD-PEG micelles under blue illumination (λ = 460 nm): (a) UV-vis spectra of FFc/PERFECTA@PFTD-PEG micelles recorded before (yellow) and after 30 s (light green) and 2 min (dark green) illumination, showing the progressive disappearance of the ferrocene absorption band; (b) photographs of PERFECTA@PFTD-PEG micelles (left), FFc/PERFECTA@PFTD-PEG micelles before illumination (middle), and FFc/PERFECTA@PFTD-PEG micelles after 10 min illumination (right).

were filled with increasing concentrations of FFc from 0 mM to 4.35 mM (5 mg mL^{-1}) in colloidal micelles (20 mg mL^{-1}), while keeping the PERFECTA concentration constant at 13.3 mM (13.5 mg mL^{-1}). ^{19}F-MRI images were acquired before and after illumination for 10 min at 460 nm, in order to determine the effect of the photo-triggered generation of ferrocenium on the relaxation times of the ^{19}F nuclei. It was expected that FFc/PERFECTA@PFTD-PEG micelles in their "On" state (before irradiation) would generate the same PERFECTA signal regardless of the FFc concentration, whereas after irradiation, signals would be attenuated by the newly formed paramagnetic ferrocenium ("Off" state).

In the absence of light, pristine FFc had moderate impact on the transverse relaxation times of the fluorine atoms of micelle-encapsulated PERFECTA. Estimated T_2 values ranged from 150 ms in the absence of FFc to 118 ms for the highest FFc concentration studied (4.35 mM). This minor variation of T_2 values did not significantly affect the recorded ^{19}F-MR images of the different tubes whose signal intensity remained nearly constant (Fig. 5a). We can thus conclude that FFc in its initial state does not interfere much with ^{19}F-MRI signals of PERFECTA, which can be readily acquired with high sensitivity using the MSME sequence.

The different tubes were then illuminated with a blue LED lamp for 10 min, and T_2 relaxation times were measured again. While the signal of sample F containing no FFc was not affected by the illumination process, a major change in T_2 values was detected for samples containing FFc and this effect was accentuated by increasing FFc concentrations (samples G and H, Fig. 5b). For example, a nearly two-fold decrease in T_2 (from 129 to 72 ms) was measured for sample G containing 0.92 mM of FFc. At the highest concentration studied ([FFc] = 4.35 mM), the FFc-derived ferrocenium induced a massive drop in T_2 from 118 to 10 ms. As a result, the ^{19}F-signal was strongly attenuated for FFc/PEFECTA@PFTD-PEG micelles exposed to light, resulting in a significant decrease in contrast. As with any MRI paramagnetic contrast agent, the impact of oxidized FFc on the transverse fluorine relaxation rate was characterized by the transverse relaxivity factor (r_2) (Fig. 5d), calculated according to the formula:

$$\frac{1/T_2 - 1/T_{2\,\mathrm{ref}}}{[\mathrm{FFc}]}$$

T_2 being the transverse relaxation time of ^{19}F nuclei in the presence of oxidized FFc and $T_{2\,\mathrm{ref}}$ the transverse relaxation time of ^{19}F nuclei in the absence of FFc. In our experiment, the transverse relaxivity factor of oxidized FFc was found to be r_2 = 22.5 mM^{-1} s^{-1}. This value is higher than that of other paramagnetic systems, such as gadolinium, a conventional MRI contrast agent (for comparison with other paramagnetic systems, see Table S1).

2.5. Preliminary biological evaluation

Prior to *in vivo* experiments, biocompatibility of the FFc/PERFECTA@PFTD-PEG micelles was assessed *in vitro*. Proliferation/survival assays were conducted on the cancerous MCF-7 cell line that was treated with the loaded carrier system and exposed or not to blue light. Under both conditions (w/and w/o illumination), no significant harmful effect on cells could be detected, even at high micelle concentration (Fig. S4). Cellular internalization of the micelles was in parallel confirmed by confocal microscopy using the fluorescent Nile Red (NR) probe as payload encapsulated in PFTD-PEG micelles (Fig. S5). We observed strong intracellular NR fluorescence signals at the vicinity of the nucleus, thus confirming effective intracellular internalization of the micellar nanocarrier. Yet, direct ^{19}F-MRI observation of FFc/PERFECTA@PFTD-PEG micelles in cells was unsuccessful as the fluorine concentration (from PERFECTA) inside of the cells was likely too low to be detected by our MRI sequence.

We nevertheless further proceeded with preliminary *in vivo* experiments. C57Bl/6 immunocompetent male mice (N = 5) were injected with FFc/PERFECTA@PFTD-PEG micelles suspended in 0.9% aqueous NaCl. A stock solution containing 13.5 mg of PERFECTA and 5 mg of FFc in 20 mg of PFTD-PEG micelles suspended in 1 mL 0.9% NaCl/H_2O was prepared and 150 μL were injected intravenously to each mouse, once a day for 3 days to ensure optimal biodistribution and ^{19}F-MRI detection. Twenty-four hours after the last injection, animals were scanned by ^{1}H/^{19}F MRI (^{1}H images were recorded for anatomical superposition). As anticipated, a clear and intense ^{19}F-signal was observed in the liver (Fig. S6), indicating nanoparticles accumulation, with [$^{19}F_{PERFECTA}$] locally reaching 43 ± 5 mM. In an attempt to quench the ^{19}F-MRI signal in the organ of interest, mice were sacrificed and their liver harvested. Given the limited tissue penetration of blue light used to convert FFc into ferrocenium, we conceived that *ex vivo* activation could offer a suitable proof of concept for attenuating PERFECTA signals in interaction with biological systems. The organ of interest was collected and a liver lobe was ground into a fine suspension to allow deeper light penetration. ^{19}F-MRI of the suspension was recorded before and after 10 min exposure to blue light. Gratifyingly, we detected a *ca.* 15% decrease in the ^{19}F-signal intensity of PERFECTA after light irradiation of the

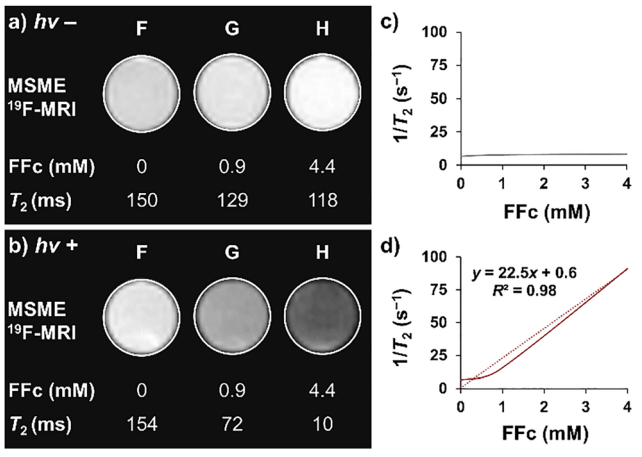

Fig. 5 Multi-Slice Multi-Echo (MSME) sequence for ^{19}F-MRI of FFc/PERFECTA@PFTD-PEG micelles incorporating variable concentrations of FFc, (a) before and (b) after illumination. Transverse relaxation rates as a function of FFc concentration, (c) before and (d) after irradiation.

sample. The partial signal attenuation was attributed to the turbidity of the ground liver sample, which likely impeded optimal photoconversion of the ferrocene moiety. Yet, this observation reflects activation of FFc into paramagnetic ferrocenium, and the subsequent acceleration of transverse relaxation rates of nearby fluorine atoms in the micelle-encapsulated PERFECTA that has accumulated in the liver.

3. Discussion

Activatable ^{19}F-MRI probes have previously been reported in the literature[31–34] and showed potential in deciphering, for example, biological processes (*e.g.* enzymatic). The vast majority of known systems rely on the "Off → On" transition.[35] A possible strategy to maintain the ^{19}F probe in an initial "Off" state can be achieved by restricting the mobility of the fluorinated probe in a rigid environment. Subsequent release of the constraint can then restore mobility and trigger the "On" state. For example, Gao and co-workers reported micelles able to detect pH transitions.[36] Block copolymers bearing fluorine atoms and amine groups were designed. These copolymers formed micelles that were initially MRI-silent due to mobility restriction. However, upon exposure to pH values below the pK_a value of the amine, micelles disassembled, thus restoring the mobility of fluorine atoms and activating the ^{19}F-MRI signal.

Another possible strategy to maintain the initial "Off" state relies on the proximity of a "silencing" paramagnetic metal center, whose separation from the ^{19}F probe can reveal MRI signals, thus switching the system to its "On" state. For example, the group of Kikuchi engineered a gadolinium (Gd) chelate linked to a fluorinated probe *via* a short peptide sequence cleavable by caspase enzymes.[37] The paramagnetic properties of Gd^{3+} ion initially attenuated the ^{19}F-MRI signal, but in the presence of active caspases, the peptide bond was cleaved, moving Gd^{3+} away from the probe and restoring the signal.

A third option to modulate MRI signals is the change in the redox state of the probe to take advantage of the paramagnetic relaxation enhancement (PRE) effect induced by metals nearby the ^{19}F nuclei. As an example, Xie *et al.* designed a copper chelate with a fluorinated side chain.[38] The fluorine atoms were initially silent in ^{19}F-NMR due to the proximity of Cu(II). However, upon reduction of paramagnetic Cu^{2+} to diamagnetic Cu^{+}, the signal was activated due to the suppression of PRE effect, thus allowing the monitoring of cellular hypoxic/normoxic conditions by ^{19}F-NMR.

In our case, and as opposed to most approaches that were previously developed in the literature, we chose to modulate the signal of PERFECTA by inducing an "On → Off" transition. Indeed, if PERFECTA-loaded micelles are to be used in cancer diagnosis with no *a priori* knowledge of the tumor location, it is difficult to envisage increasing the local MRI contrast in the pathological zone by externally turning-on the probe. Yet, contrast can be enhanced by selectively turning-off the interfering signals present in a well-defined organ such as the liver.

To turn-off the signal of PERFECTA-loaded micelles, we co-encapsulated a redox active modulator of the MRI signal in the form of a fluorophilic ferrocene derivative (FFc). FFc is photo-responsive and can undergo oxidation to ferrocenium upon illumination at a suitable wavelength (*i.e.* 460 nm). In the absence of light, the ferrocene derivative is in its diamagnetic state and does not disturb the signal of PERFECTA. This corresponds to the initial "On" state of the probe that can be readily visualized by ^{19}F-MRI. However, when light is applied, FFc is photo-oxidized into paramagnetic ferrocenium, which results in reduction of the spin–spin relaxation times ($T_2 \rightarrow 0$) and broadening/attenuation of the ^{19}F signals of PERFECTA. In our experiments, a strong decrease of the T_2 of PERFECTA, from 118 to 10 ms, was observed at the highest FFc concentration studied (4.35 mM), together with a significant attenuation of the MRI signal. This corresponds to the "Off" state of the probe due to the generation of paramagnetic iron that triggers a PRE effect. This phenomenon is due to dipolar interactions between unpaired electrons of ferrocenium ions and nuclear spins of ^{19}F atoms, leading to accelerated transverse relaxation rates of the latter (shorter T_2 relaxation times) and hence lowering ^{19}F-MRI signal in T_2 weighted images.[38,39]

To the best of our knowledge, there are only two other examples in the literature of ferrocene-based systems for modulating the ^{19}F-magnetic resonance signals. Ferrocene-functionalized fluorinated dendrimers were synthesized by the group of Chujo as redox-responsive ^{19}F-NMR probes.[40] Chemical oxidation of the ferrocenyl unit by ammonium persulfate led to the formation of the ferrocenium cation. The latter induced a PRE effect to the adjacent fluorine nuclei, leading to a significant decrease in ^{19}F-NMR signal intensity. Chemical reduction of the ferrocenium cation back to ferrocene resulted in the recovery of the ^{19}F-NMR signal. Yet, this system was not applied to magnetic resonance imaging. The second example is from the team of Hruby,[41] who investigated polymers incorporating fluorinated ferrocene derivatives that were treated under ammonium peroxydisulfate/$CuCl_2$ as the oxidant system. This permitted the conversion of the diamagnetic ferrocene moiety into paramagnetic ferrocenium, which markedly changed the chemical shift and relaxation time of the ^{19}F nuclei, as visualized by ^{19}F-MRI.

Here, we used light-activation of the ferrocenyl unit, which is unprecedented in MRI. In addition, our system enables signals from the fluorinated probe to be disabled, which has only been scarcely explored in the literature as most of the current approaches deal with turn-on probes. The latter strategy, when externally activated, cannot be used in the context of cancer diagnosis without prior knowledge of the tumor location. In that sense, our nanoscale platform, combining MRI-responsive PERFECTA and photo-activatable FFc in a biocompatible micelle, could provide images with enhanced contrast in targeted tumors, by selectively quenching the MRI signal in anatomically defined satellite organs, such as the liver. Yet, a preliminary proof of concept could be achieved *ex vivo*, but we still have to solve the problem of the activation wavelength of FFc, which needs to be shifted towards the near-infrared region for better light penetration into deep tissues. A potential strategy could be the co-encapsulation of upconverting nanoparticles, which convert low-energy near-infrared photons into

higher-energy photons capable of inducing ferrocene photo-oxidation – a direction currently under investigation.

4. Conclusion

A photo-responsive ferrocenyl unit was designed to extinguish the ^{19}F-MRI signal of PERFECTA encapsulated in PFTD-PEG micelles. Upon activation by light, FFc is photo-oxidized into the corresponding ferrocenium having paramagnetic properties and locally attenuating MRI signals through PRE effect. Micellar co-encapsulation of the photo-activatable quencher and the superfluorinated probe provided the necessary proximity and confinement for PRE-mediated ^{19}F signal silencing. This strategy allows full spatial and temporal control of MRI responses that can be turned off on demand in areas not to be imaged, while maintaining a clear signal in the area of interest. A nearly twelve-fold decrease was measured for the T_2 relaxation time of ^{19}F-PERFECTA (from 118 to 10 ms) at the highest FFc concentration studied (4.35 mM). This decrease was accompanied with a significant attenuation of the MRI signal. Given that the pharmacokinetic and tumor-targeting properties of PFTD-PEG micelles have already been favorably evaluated by our group in mouse models, it is reasonable to assume that FFc/PERFECTA@PFTD-PEG micelles could soon find applications for preclinical *in vivo* tumor diagnosis, with a reduction of interfering signals where appropriate.

5. Experimental

Detailed experimental procedures can be found in the SI. All *in vivo* experiments were conducted in strict accordance with the recommendations of the European Community (2010/63/EU) and the French legislation (decree no. 2013-118) for use and care of laboratory animals. Experimental protocols were approved by the ''Comité d'Éthique en Expérimentation Animale du Commissariat à l'Énergie Atomique et aux Énergies Alternatives – Direction des Sciences du Vivant Ile-de-France'' (CETEA/CEA/DSV IdF, protocol number APAFIS #33809-2021110817536958).

Author contributions

Investigation: C. L., G. P., M. V., M. G., E. S., F. G., S. M.; methodology: S. M., E. G., E. D.; conceptualization: E. G., E. D.; supervision: S. M., E. G., E. D.; writing – original draft: E. D.; writing – review & editing: G. P., S. M., E. G., E. D.

Conflicts of interest

There are no conflicts to declare.

Data availability

The data supporting this article have been included as part of the supplementary information (SI). Supplementary information is available. See DOI: **https://doi.org/10.1039/d5nh00468c**.

Acknowledgements

The ''Service de Chimie Bioorganique et de Marquage'' (SCBM) is a partner of NOMATEN, a Centre of Excellence in Multifunctional Materials for Industrial and Medical Applications (EU H2020 Teaming #857470).

Notes and references

1 S. Posse, R. Otazo, S. R. Dager and J. Alger, *J. Magn. Reson. Imaging*, 2013, **37**, 1301.
2 H. K. Kim, G. H. Lee and Y. Chang, *Future Med. Chem.*, 2018, **10**, 639.
3 Z. Y. Shen, A. G. Wu and X. Y. Chen, *Mol. Pharm.*, 2017, **14**, 1352.
4 G. Wang, H. Yang, J. Li, J. Wen, K. Zhong and C. Tian, *Magn. Reson. Lett.*, 2023, **3**, 327.
5 I. Tirotta, V. Dichiarante, C. Pigliacelli, G. Cavallo, G. Terraneo, F. Baldelli Bombelli, P. Metrangolo and G. Resnati, *Chem. Rev.*, 2015, **115**, 1106.
6 R. K. Harris, E. D. Becker, S. M. Cabral de Menezes, R. Goodfellow and P. Granger, *Solid State Nucl. Magn. Reson.*, 2002, **22**, 458.
7 B. L. Bona, O. Koshkina, C. Chirizzi, V. Dichiarante, P. Metrangolo and F. Baldelli Bombelli, *Acc. Mater. Res.*, 2023, **4**, 71.
8 I. Tirotta, A. Mastropietro, C. Cordiglieri, L. Gazzera, F. Baggi, G. Baselli, M. G. Bruzzone, I. Zucca, G. Cavallo, G. Terraneo, F. Baldelli Bombelli, P. Metrangolo and G. Resnati, *J. Am. Chem. Soc.*, 2014, **136**, 8524.
9 C. Chirizzi, C. Morasso, A. A. Caldarone, M. Tommasini, F. Corsi, L. Chaabane, R. Vanna, F. Baldelli Bombelli and P. Metrangolo, *J. Am. Chem. Soc.*, 2021, **143**, 12253.
10 C. Chirizzi, L. Gatti, M. Sancho-Albero, V. Sebastian, M. Arruebo, L. Uson, G. Neri, J. Santamaria, P. Metrangolo, L. Chaabane and F. Baldelli Bombelli, *Colloids Surf., B*, 2022, **220**, 112932.
11 N. Ayaz, V. Dichiarante, C. Pigliacelli, J. Repossi, L. Gazzera, M. Boreggio, D. Maiolo, C. Chirizzi, G. Bergamaschi, L. Chaabane, E. Fasoli, P. Metrangolo and F. Baldelli Bombelli, *Adv. Mater. Interfaces*, 2022, **9**, 2101677.
12 M. Sancho-Albero, N. Ayaz, V. Sebastian, C. Chirizzi, M. Encinas-Gimenez, G. Neri, L. Chaabane, L. Luján, P. Martin-Duque, P. Metrangolo, J. Santamaría and F. Baldelli Bombelli, *ACS Appl. Mater. Interfaces*, 2023, **15**, 8974.
13 E. Gravel, J. Ogier, T. Arnauld, N. Mackiewicz, F. Ducongé and E. Doris, *Chem. – Eur. J.*, 2012, **18**, 400.
14 P. Anilkumar, E. Gravel, I. Theodorou, K. Gombert, B. Thézé, F. Ducongé and E. Doris, *Adv. Funct. Mater.*, 2014, **24**, 5246.
15 I. Theodorou, P. Anilkumar, B. Lelandais, D. Clarisse, A. Doerflinger, E. Gravel, F. Ducongé and E. Doris, *Chem. Commun.*, 2015, **51**, 14937.
16 A. Doerflinger, N. N. Quang, E. Gravel, G. Pinna, M. Vandamme, F. Ducongé and E. Doris, *Chem. Commun.*, 2018, **54**, 3613.
17 J. Alliot, I. Theodorou, D. V. Nguyen, C. Forier, F. Ducongé, E. Gravel and E. Doris, *Nanoscale*, 2019, **11**, 9756.
18 M. D. Hoang, M. Vandamme, G. Kratassiouk, G. Pinna, E. Gravel and E. Doris, *Nanoscale Adv.*, 2019, **1**, 4331.

19 J. Alliot, I. Theodorou, F. Ducongé, E. Gravel and E. Doris, *Chem. Commun.*, 2019, **55**, 14968.
20 F. Costamagna, H. Hillaireau, J. Vergnaud, D. Clarisse, L. Jamgotchian, O. Loreau, S. Denis, E. Gravel, E. Doris and E. Fattal, *Nanoscale*, 2020, **12**, 2452.
21 E. Porret, S. Hoang, C. Denis, E. Doris, M. Hruby, A. Novell, E. Gravel and C. Truillet, *Nanoscale*, 2023, **15**, 12574.
22 L. Jamgotchian, L. Devel, R. Thai, L. Poupel, T. Huby, E. Gautier, W. Le Goff, P. Lesnik, E. Gravel and E. Doris, *Nanoscale*, 2023, **15**, 18864.
23 S. Godel-Pastre, E. Porcel, C. Denis, C. Leterrier, E. Doris, C. Truillet and E. Gravel, *ACS Appl. Mater. Interfaces*, 2024, **16**, 21557.
24 E. Gravel, C. Demeese and E. Doris, *Synlett*, 2024, **35**, 1954.
25 L. Jamgotchian, S. Vaillant, E. Selingue, A. Doerflinger, A. Belime, M. Vandamme, G. Pinna, W. L. Ling, E. Gravel, S. Mériaux and E. Doris, *Nanoscale*, 2021, **13**, 2373.
26 D. E. Owens and N. A. Peppas, *Int. J. Pharm.*, 2006, **307**, 93.
27 A. M. Tarr and D. M. Wiles, *Can. J. Chem.*, 1968, **46**, 2725.
28 L. Zhang, X. Gao, L. Yang, P. Yu and L. Mao, *ACS Appl. Mater. Interfaces*, 2013, **5**, 8120.
29 S. Hoang, M. Vandamme, G. Pinna, F. Miserque, P. Stepanek, E. Doris, M. Hruby and E. Gravel, *ACS Appl. Mater. Interfaces*, 2024, **16**, 5666.
30 Y. Yamaguchi and C. Kutal, *Inorg. Chem.*, 1999, **38**, 4861.
31 M. Carril, *J. Mater. Chem. B*, 2017, **5**, 4332.
32 J. Salaam, M. Minoshima and K. Kikuchi, *Anal. Sens.*, 2023, **3**, e202200081.
33 H. Lin, X. Tang, A. Li and J. Gao, *Adv. Mater.*, 2021, **33**, 2005657.
34 W. C. Geng, Z. Zheng and D. S. Guo, *View*, 2021, **2**, 20200059.
35 X. Zhu, P. Zhang, D. Liu, L. Tao, J. Du and X. Gao, *Trends Anal. Chem.*, 2024, **172**, 117607.
36 X. Huang, G. Huang, S. Zhang, K. Sagiyama, O. Togao, X. Ma, Y. Wang, Y. Li, T. C. Soesbe, B. D. Sumer, M. Takahashi, A. D. Sherry and J. Gao, *Angew. Chem., Int. Ed.*, 2013, **52**, 8074.
37 S. Mizukami, R. Takikawa, F. Sugihara, Y. Hori, H. Tochio, M. Walchli, M. Shirakawa and K. Kikuchi, *J. Am. Chem. Soc.*, 2008, **130**, 794.
38 D. Xie, M. Yu, R. T. Kadakia and E. L. Que, *Acc. Chem. Res.*, 2020, **53**, 2.
39 L. Helm, *Prog. Nucl. Magn. Reson. Spectrosc.*, 2006, **49**, 45.
40 K. Tanaka, N. Kitamura, Y. Takahashi and Y. Chujo, *Bioorg. Med. Chem.*, 2009, **17**, 3818.
41 P. Švec, O. V. Petrov, J. Lang, P. Štěpnička, O. Groborz, D. Dunlop, J. Blahut, K. Kolouchová, L. Loukotová, O. Sedláček, T. Heizer, Z. Tošner, M. Šlouf, H. Beneš, R. Hoogenboom and M. Hrubý, *Macromolecules*, 2022, **55**, 658.